

Structural Determinants of RXPA380, a Potent and Highly Selective Inhibitor of the Angiotensin-Converting Enzyme C-Domain

Dimitris Georgiadis,[‡] Philippe Cuniasse,[§] Joël Cotton,[§] Athanasios Yiotakis,[‡] and Vincent Dive^{*§}

Département d'Ingénierie et d'Etudes des Protéines, CEA, 91191 Gif/Yvette Cedex, France, and Laboratory of Organic Chemistry, Department of Chemistry, University of Athens, Panepistimiopolis Zografou, 15771 Athens, Greece

Received March 12, 2004; Revised Manuscript Received April 27, 2004

ABSTRACT: RXPA380 (Cbz-PheΨ[PO₂CH]Pro-Trp-OH) was reported recently as the first highly selective inhibitor of the C-domain of somatic angiotensin-converting enzyme (ACE), able to differentiate the two active sites of somatic ACE by a selectivity factor of more than 3 orders of magnitude. The contribution of each RXPA380 residue toward this remarkable selectivity was evaluated by studying several analogues of RXPA380. This analysis revealed that both pseudo-proline and tryptophan residues in the P₁' and P₂' positions of RXPA380 play a critical role in the selectivity of this inhibitor for the C-domain. This selectivity is not due to a preference of the C-domain for inhibitors bearing pseudo-proline and tryptophan residues, but rather reflects the poor accommodation of these inhibitor residues by the N-domain. A model of RXPA380 in complex with the ACE C-domain, based on the crystal structure of germinal ACE, highlights residues that may contribute to RXPA380 selectivity. From this model, striking differences between the N- and C-domains of ACE are observed for residues defining the S₂' pocket. Of the twelve residues that surround the tryptophan side chain of RXPA380 in the C-domain, five are different in the N-domain. These differences in the S₂' composition between the N- and C-domains are suggested to contribute to RXPA380 selectivity. The structural insights provided by this study should enhance understanding of the factors controlling the selectivity of the two domains of somatic ACE and allow the design of new selective ACE inhibitors.

Angiotensin-converting enzyme (ACE) in vertebrates is a zinc metallopeptidase involved in the release of angiotensin II and the inactivation of bradykinin, two peptide hormones that play a key role in the regulation of blood pressure and renal and cardiovascular functions (1–4). ACE inhibitors have been on the market for more than 20 years, with successful applications ranging from mild hypertension to postmyocardial infarction (5, 6). Somatic ACE contains two active sites (7, 8), and most of the currently available inhibitors used in clinical practice interact with these two active sites to a similar extent (6). On the basis of these facts, we previously proposed to develop inhibitors able to differentiate these two active sites, as a new generation of ACE inhibitors. The first N-domain-specific inhibitor of ACE, RXP407, was identified by screening phosphinic peptide libraries (9). A C-domain-specific inhibitor of ACE, RXPA380, was recently reported (10). In vivo experiments demonstrated that with these two novel domain-specific ACE inhibitors it is possible to prevent the angiotensin I conversion without affecting bradykinin cleavage (10). Thus, such ACE inhibitors may find new therapeutic applications in the control of diseases mediated mainly by angiotensin II overproduction, such as atherosclerosis (11). Since these studies, the 3D crystal structure of germinal ACE in complex with lisinopril inhibitor has been solved (12). Germinal ACE

has only one active site, which corresponds to the C-domain of somatic ACE (13). In this study, the structural requirements for the remarkable selectivity displayed by RXPA380 were determined by developing several analogues of this compound. Using the germinal ACE structure, the binding of RXPA380 was modeled into the C-domain. This model offers a structural basis to tentatively explain RXPA380 selectivity.

MATERIAL AND METHODS

Enzymes. N-domain and C-domain mutants of human recombinant ACE have been described (8). The term C-domain mutant describes an ACE form in which the N-domain was inactivated. N-domain mutant corresponds to an ACE in which the C-domain was inactivated.

Enzyme Assays and Inhibition Studies. *K_i* values reported in Table 1 were determined using, respectively, ACE C-domain mutant (*K_i*(C)) and ACE N-domain mutant (*K_i*(N)). *K_i* values were determined as described (14). Enzyme and inhibitors were incubated for 45 min before the initiation of the reaction by substrate addition. Assays were performed at 25 °C in 50 mM Hepes (pH 6.8), 200 mM NaCl, and 10 μM ZnCl₂. Continuous assays with the fluorogenic substrate Mca-Ala-Ser-Asp-Lys-Dpa-OH¹ were performed as previously described (14).

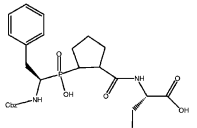
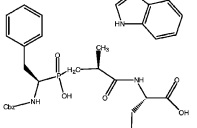
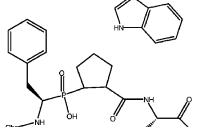
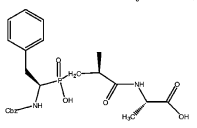
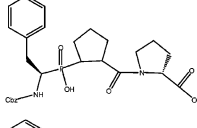
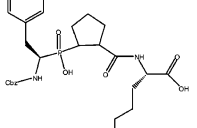
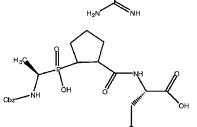
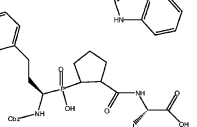
Compound Synthesis. Synthesis of inhibitor RXPA380, (2*S*)-2-[(2-[(1*R*)-1-[(benzyloxy)carbonyl]amino]-2-phenylethyl)(hydroxy)phosphinyl]cyclopentyl]carbonyl-amino]-3-(1*H*-indol-3-yl)propionic acid (Cbz-PheΨ[P(O)-

* To whom correspondence should be addressed. Phone: 33 1 69083585. Fax: 33 1 69089071. E-mail: vincent.dive@cea.fr.

[‡] University of Athens.

[§] CEA.

Table 1: Selectivity of RXPA380 Analogues toward ACE C- and N-Domain Mutant

Compounds N°	Ki C	Ki N nM	Selectivity Ki N/C
RXPA380			
	3	10000	3300
7			
	0.5	45	90
8			
	20	450	22
9			
	0.8	0.8	1
10			
	4	60	15
11			
	9	200	22
12			
	60	8000	130
13			
	65	9000	138

(OH)CH]Pro-Trp-OH), is shown in Scheme 1. The aminophosphinic analogue of phenylalanine, **1**, was synthesized and its enantiomeric resolution performed according to the protocol of Baylis (15).

A mixture of (*R*)-aminophosphinic acid **1** (3.19 g, 10 mmol) and HMDS (6.3 mL, 30 mmol) was flushed by Ar and heated at 110 °C for 3 h. At this temperature, 5-acetoxycyclopent-1-enecarboxylic acid ethyl ester (**2**) (2.38 g 12 mmol) was added, and the resulting solution was stirred for 4 h at 90 °C. Then, the mixture was cooled at 70 °C, absolute

EtOH (10 mL) was added dropwise, and the resulting mixture was stirred at 70 °C for 30 min. The solvents were evaporated, and the residue was dissolved in 5% NaHCO₃ (15 mL) and hexane (15 mL). The organic phase was separated, and the aqueous phase was washed twice with hexane (2 × 15 mL). The aqueous phase was acidified with 1 M HCl to pH 1 and saturated with NaCl. Extractions with AcOEt (3 × 5 mL) followed, and the crude product was obtained after evaporation of the solvents. Purification by silica gel chromatography (70–230 mesh), using chloroform/methanol/acetic acid, (7:0.3:0.3) as eluent, afforded 4.07 g (yield 89%) of pseudo-dipeptide 5-[(1*R*)-1-[(benzyloxy)carbonyl]amino]-2-phenylethyl(hydroxy)phosphinyl]-cyclopent-1-ene-1-carboxylic acid, ethyl ester (**3**) as a white solid: ³¹P NMR (81 MHz, *d*₆-DMSO) δ 46.45, 47.41.

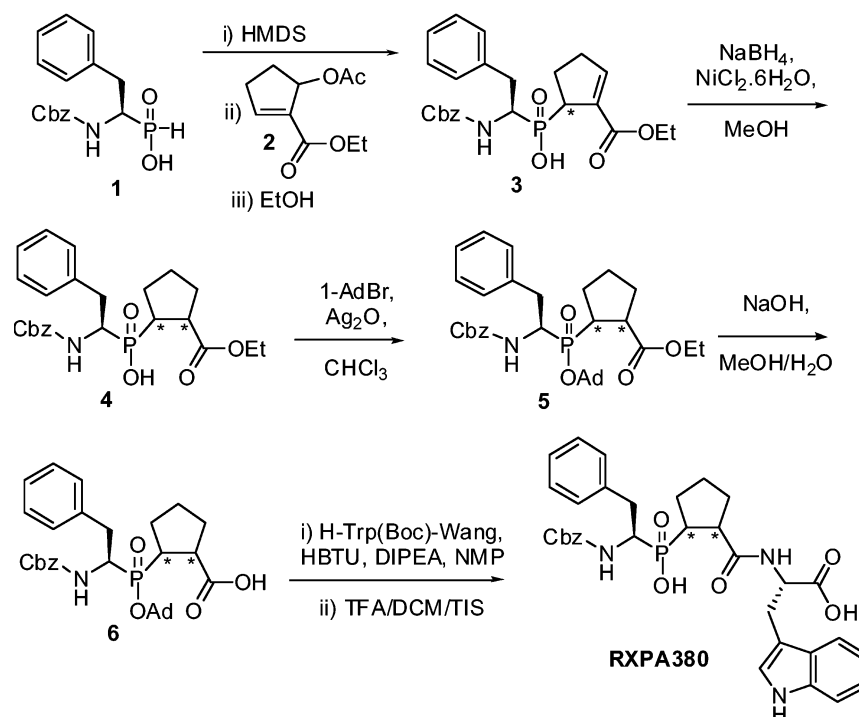
To a solution of pseudo-dipeptide **3** (1.37 g, 3 mmol) and NiCl₂·6H₂O (1.07 g, 9 mmol) in THF (12 mL) and MeOH (7.5 mL) was added NaBH₄ (0.56 g, 15 mmol) portionwise for 30 min at −30 °C. Then, the mixture was stirred at −30 °C for 10 min. After the end of the reaction time, the mixture was evaporated and the residue was partitioned with AcOEt (25 mL) and 1 N HCl (20 mL) (to pH 1). The organic phase was separated, washed with H₂O (10 mL), and dried with Na₂SO₄. The crude product was purified by silica gel chromatography (70–230 mesh), using chloroform/methanol/acetic acid (7:0.3:0.3). After purification, 1.25 g (yield 91%) of phosphinate 2-[(1*R*)-1-[(benzyloxy)carbonyl]amino]-2-phenylethyl(hydroxy)phosphinyl]cyclopentanecarboxylic acid, ethyl ester (**4**) was obtained as a white solid: ³¹P NMR (81 MHz, *d*₆-DMSO) δ 45.99, 46.21, 48.87, 49.27.

To a refluxing solution of phosphinate **4** (0.92 g, 2 mmol) and 1-adamantyl bromide (0.65 g, 3 mmol) in CHCl₃ (20 mL) was added silver(I) oxide (0.56 g, 2.4 mmol) portionwise over 1 h. After the solution was refluxed for 24 h, the solvent was removed in vacuo and the residue was treated with Et₂O (10 mL). The resulting mixture was filtered through Celite, and the filtrates were evaporated. The residue was purified by silica gel chromatography (70–230 mesh), using CHCl₃/*i*-PrOH (9.8:0.2) as eluent. After purification, 1.05 g (yield 89%) of phosphinate 2-[(1*R*)-1-[(benzyloxy)carbonyl]amino]-2-phenylethyl(adamantyl)phosphinyl]-cyclopentanecarboxylic acid, ethyl ester (**5**) were afforded as a colorless gum: ³¹P NMR (81 MHz, *d*₆-DMSO) δ 49.00, 49.35, 49.42, 49.72, 51.32, 51.45, 52.94, 53.54.

To a stirred solution of fully protected pseudo-dipeptide **5** (0.47 g, 0.8 mmol) in MeOH (5 mL) was added a 4 M aqueous solution of NaOH (0.7 mL) dropwise. The reaction mixture was stirred for 2 h. Then the solvent was removed, and the residue was diluted with water and acidified with 0.5 M HCl in an ice–water bath. This aqueous solution was extracted with AcOEt (2 × 10 mL), and the combined organic layers were dried over Na₂SO₄ and concentrated. The residue was purified by silica gel chromatography (70–230 mesh), using CHCl₃/MeOH (9.6:0.4) as eluent. After purification, 0.42 g (yield 94%) of building block 2-[(1*R*)-1-[(benzyloxy)carbonyl]amino]-2-phenylethyl(adamantyl)phosphinyl]-cyclopentanecarboxylic acid (**6**) was afforded as a white solid: ³¹P NMR (81 MHz, *d*₆-DMSO) δ 51.07, 51.54, 51.77, 52.28, 53.02, 53.33.

Fmoc-Trp(Boc)-Wang resin (0.2 mmol) was suspended in NMP (3 mL), and the solvent was removed after 15 min of

¹ Abbreviations: HMDS, 1,1,1,3,3,3-hexamethyldisilazane; NMP, 1-methyl-2-pyrrolidinone; HBTU, *O*-benzotriazol-1-yl-*N,N,N',N'*-tetramethyluronium hexafluorophosphate; TFA, trifluoroacetic acid; Cbz, carbobenzyloxy; DCM, dichloromethane; DIPEA, *N,N*-diisopropylethylamine; TIS, triisopropylsilane; Et, ethyl; Ac, acetyl; THF, tetrahydrofuran; DMSO, dimethyl sulfoxide; Me, methyl; Boc, *N*-tert-butoxycarbonyl; Ad, adamantyl; Mca, (7-methoxycoumarin-4-yl)acetyl; Dpa, *N*³-(2,4-dinitrophenyl)-*L*-2,3-diaminopropionyl.

Scheme 1^a

^a Reagents and conditions: (i) HMDS (3 equiv), 110 °C, 3 h, then **2** (1.2 equiv), 90 °C, 4 h, then EtOH, 70 °C, 15 min, 89%. (ii) NaBH₄ (5 equiv), NiCl₂ (3 equiv), MeOH, −30 °C, 30 min, 91%. (iii) 1-AdBr (1.5 equiv), Ag₂O (1.2 equiv), CHCl₃, 24 h, reflux, 89%. (iv) 0.5 N NaOH/MeOH, 12 h, rt, 94%. (v) H₂N-Trp(Boc)-Wang (0.9 equiv), DIPEA (9 equiv), HBTU (3 equiv), NMP, 24 h, rt. (vi) TFA/CH₂Cl₂/H₂O/(*i*-Pr)₃SiH (90:7.5:1.25:1.25), 3 h, rt.

shaking. The resin was treated with a solution of 20% piperidine in NMP (2 × 5 mL) for 15 min and was then filtered and washed successively with NMP (7 × 5 mL), CH₂Cl₂ (3 × 5 mL), and Et₂O (2 × 5 mL). NMP (1 mL), diisopropylethylamine (0.35 mL, 2 mmol), phosphinic tripeptide **6** (0.22 mmol) dissolved in 1 mL of NMP, and HBTU (228 mg, 0.6 mmol) dissolved in NMP (1.5 mL) were added to the resin, and the reactor was shaken for 24 h. After filtration and successive washings with NMP (4 × 5 mL) and CH₂Cl₂ (5 × 5 mL), the resin was treated with 5 mL of TFA/CH₂Cl₂/H₂O/(*i*-Pr)₃SiH (90:7.5:1.25:1.25) for 3 h at room temperature. Filtration and evaporation of the filtrates afforded the crude product which was purified and separated into four diastereoisomers by RP-HPLC (SPPS yield 96%, purity (decided by HPLC) 63%). RXPA380, the active component of the above diastereoisomeric mixture, corresponds to the first eluted fraction in RP-HPLC and to 40% of the total amount of tripeptide (*t*_R = 29.74 min; gradient *t* = 0 min (65% A, 35% B), *t* = 23 min (65% A, 35% B), *t* = 40 min (60% A, 40% B); solvent A = 0.1% TFA and 10% CH₃CN in H₂O; solvent B = 0.1% TFA and 90% CH₃CN in H₂O): ¹H NMR (250 MHz, *d*₆-DMSO) δ 1.39–1.67 (m, 2H, CH₂CH₂CH₂), 1.68–1.90 (m, 4H, CH₂CH₂CH₂), 2.41–2.59 (m, 1H, PCH Pro), 2.67–2.87 (m, 1H, CHCHHPh), 2.96–3.27 (m, 4H, CHCHHPh, PCHCH Pro, CHCH₂-Ar Trp), 3.91–4.10 (m, 1H, NCHP Phe), 4.42–4.58 (m, 1H, NCH Trp), 4.93 (dd, 2H, *J* = 12.9, 21.7 Hz, OCH₂Ph), 6.90–7.42 (m, 15H, aryl), 7.56 (s, 1H, NH Trp), 7.65 (d, 1H, ³J_{HH} = 13.7 Hz, NH Phe), 8.31 (d, 1H, ³J_{HH} = 9.7 Hz, NH indole); ¹³C NMR (63 MHz, *d*₆-DMSO) δ 27.6 CH₂CH₂CH₂), 28.3 (CH₂ Trp), 28.6 (PCHCH₂), 32.5 (PCHCHCH₂), 34.6 (CH₂ Phe), 39.4 (³J_{CP} = 103 Hz, PCH Pro), 45.4 (PCHCH Pro), 52.8 (³J_{CP} = 94 Hz, NCHP Phe), 54.4 (NCH Trp), 66.3

(OCH₂), 110.7, 112.5, 119.2, 122.0, 124.9, 127.3, 127.8, 128.4, 128.7, 129.3, 129.4, 130.2, 137.2, 138.3, 139.4 139.6 (aryl), 157.0 (OCONH), 174.6 (CCONH), 175.1 (COOH); ³¹P NMR (101 MHz, *d*₆-DMSO) δ 53.8; ESMS *m/z* calcd for C₃₃H₃₇N₃O₇P (M + H)⁺ 617.2, found 617.3.

RXPA380 analogues **8**, **10**, and **11** were prepared and isolated similarly to RXPA380 by using building block Cbz-PheΨ[P(O)(OAd)CH]Pro-OH (**6**). For the synthesis of RXPA380 analogues **12** and **13**, the preparation of phosphinic precursors Cbz-AlaΨ[P(O)(OAd)CH]Pro-OH and Cbz-hPheΨ[P(O)(OAd)CH]Pro-OH was required. The synthesis of these adamantyl phosphinates was carried out according to the procedure described above for building block **6**, starting from the Cbz-protected aminophosphinic analogues of alanine and homophenylalanine, respectively. Finally, pseudo-tripeptides **7** and **9** were prepared according to our previously published methodology (16). Each diastereoisomer of pseudo-tripeptides presented in Table 1 was found to be correct by MS analysis. Further spectroscopic and analytical data of all new pseudo-proline phosphinic synthetic intermediates are supplied as Supporting Information.

Molecular Modeling. The molecular model of the interaction of the phosphinic inhibitor RXPA380 with the catalytic C-domains of ACE, based on 3D structures of the germinal form of this enzyme complexed with lisinopril (PDB code 1O86) (12), was achieved with the program CHARMM (version 27) (17). We used the CHARMM force field version 22 (18). The geometrical and nonbonded parameters for the phosphinic inhibitor were derived from ab initio quantum calculations with the program GAUSSIAN98 (19). These calculations were done at the MP2 level of theory using a 6-31+G(d,p) basis set.

An initial model of RXPA380 was built with the InsightII software (Accelrys Inc.) The initial position of RXPA380 in the catalytic C-domain of ACE was obtained by superimposing the main chain of the phosphinic inhibitor on the corresponding atoms of lisinopril in the structure of this molecule complexed with the germinal form of ACE. This starting structure of the complex RXPA380–C-domain of ACE was then refined by energy minimization and molecular dynamics with CHARMM. To preserve the structure of the protein during the relaxation of the complex, harmonic restraints were applied to the atomic positions of several sets of atoms. The harmonic constants were set to 100, 5, and 0.5 kcal mol⁻¹ Å⁻² for the ions and their chelating residues, the atoms and the residues of the protein situated at a distance greater than 5 Å from the inhibitor, and the atoms of the inhibitor and those of the residues of the protein at a distance lower than 5 Å, respectively. The initial step of the relaxation protocol consists of an initial 2000 cycle of adopted basis Newton–Raphson energy minimization. Then 100 000 steps of molecular dynamics using the Verlet algorithm were undertaken. The integration step was set to 0.0005 ps. The temperature was gradually increased by 25 K each 1000 steps to reach 300 K. This molecular dynamics run was followed by 5000 cycles of energy minimization. The resulting structure was then analyzed. During the calculations, the nonbonded interactions were modeled using a Lennard-Jones function and a Coulombic electrostatic term with a non-bonded cutoff of 13 Å. The dielectric constant was set to 1.

RESULTS AND DISCUSSION

Chemistry. The classical approach to the preparation of phosphinic peptides, based on the Michael addition of a nucleophilic phosphonite to the appropriate acrylate, did not allow preparation of Cbz-PheΨ[P(O)(OH)CH]Pro-OEt (compound **4**, Scheme 1), an intermediate required to synthesize RXPA380. These negative results have led us to develop a new strategy, outlined in Scheme 1. This strategy relies on the use of allylic acetate **2**, instead of an acrylate, as an electrophilic synthon which presents an enhanced reactivity toward the Michael addition of phosphonite **1**. This procedure gave high yields of the Cbz-Ψ[P(O)(OH)CH]dehydro-Pro-OEt synthon (**3**). After the chemoselective hydride reduction of the double bond in **3**, compound **4** was obtained as a mixture of four diastereoisomers. Interestingly, ³¹P NMR analysis of this mixture revealed the presence of two pairs of peaks in the spectrum, at a ratio of ~70:30. This ratio implies that a certain regioselectivity occurs during hydride addition in **3** that leads to an excess of the less crowded anti isomers of **4**, as compared to the syn isomers, an effect that has previously been observed in similar 1,4-unsaturated substrates when nickel boride is used as the reduction agent (20). The same ratio between the different diastereoisomers was also observed in the HPLC profile of Cbz-PheΨ[P(O)(OH)CH]Pro-Trp-OH, with the active diastereoisomer (RXPA380) corresponding to 40% of the total tripeptide quantity. Full spectroscopic data for RXPA380 are quoted in the Supporting Information.

Inhibitor Selectivity and Potency. Compounds reported in Table 1 were obtained as a mixture of either two or four diastereoisomers (compounds containing a pseudo-proline) easily resolved by RP-HPLC. Evaluation of the inhibitory potency of these HPLC fractions revealed that, in each case,

the fraction eluting first was the only one endowed with inhibitory potency. Interestingly, initial modeling studies of RXPA380 showed that only one diastereoisomer of this compound can be easily accommodated in the active site of the germinal form of ACE. Furthermore, this diastereoisomer of RXPA380 can be superimposed on the structure that lisinopril adopts in complex with ACE (see below). In this diastereoisomer, carbons α and ε of the pseudo-proline residue possess the *S* and *R* configurations, respectively. The pseudo-proline-containing compounds reported in Table 1 are presumed to have the same configuration. Those containing a pseudo-alanine should possess the *S* configuration at the level of the pseudo-alanine residue. This absolute requirement for potency of the *S* configuration for the P₁' residue of ACE inhibitors has been reported previously (21).

Replacement of either pseudo-proline or tryptophan residues in RXPA380 resulted in compounds (**7** and **8**) that are less selective, as compared to RXPA380. This loss in selectivity is mostly explained by the potency of these two compounds toward the N-domain of ACE. Compounds **7** and **8** inhibit the N-domain more potently than RXPA380. The role of pseudo-proline and tryptophan in the selectivity is further demonstrated by compound **9**, which is a highly potent, but nonselective, inhibitor of ACE. Altogether, these data demonstrate that pseudo-proline and tryptophan residues in RXA380 are rather well accommodated by the C-domain active site, while they are much less tolerated by the N-domain active site. The role of tryptophan in the specificity is further outlined by compounds **10** and **11**, two compounds that are less specific than RXPA380. Compounds **12** and **13** are poor inhibitors of the N-domain, confirming the detrimental role of the pseudo-proline and tryptophan residues for N-domain binding. However, these two compounds also display a weaker potency toward the C-domain, as compared to RXPA380, an effect that reduces their selectivity. These results show that the C-domain of ACE exhibits a preference for a pseudo-phenylalanine residue in the inhibitor P₁ position, as compared to a pseudo-alanine or pseudo-homo-phenylalanine.

ACE C-Domain–RXPA380 Model. The model of interaction of RXPA380 in the C-domain ACE active site was based on the crystal structure of lisinopril in complex with germinal ACE. One remarkable feature of the bound conformation of lisinopril in this complex concerns the values of the φ and ψ angles adopted by the lysine residue, respectively, –61° and 149°. Such values explain the bent conformation of lisinopril in the ACE active site (Figure 1). Interestingly, these values correspond to the φ and ψ values observed in the standard proline residue. This explains why the pseudo-proline of RXPA380 can replace the lysine residue of lisinopril without particular conformational adjustment (Figure 1). This bent conformation places the free carboxylate of lisinopril in a favorable orientation for interacting through hydrogen bonding with the Lys⁵¹¹ and Tyr⁵²⁰ side chains of ACE. This remarkable conformation of lisinopril also explains why, of the four diastereoisomers of RXPA380, only one could be superimposed on the lisinopril-bound conformation and as well why only one diastereoisomer of RXPA380 displayed potency.

The RXPA380–ACE model revealed the residues that surrounded both the pseudo-proline and tryptophan of RXPA380, the two critical residues of the inhibitor that

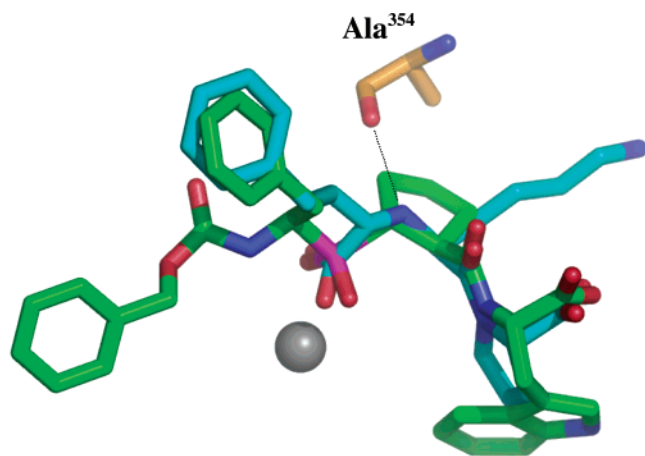


FIGURE 1: Superimposition of the structure of RXPA380 (carbon atoms in green) with the structure that lisinopril (carbon atoms in cyan) adopts in the complex with germinal ACE (PDB code 1O86). Hydrogen atoms are omitted. The figure was prepared with PyMOL software.

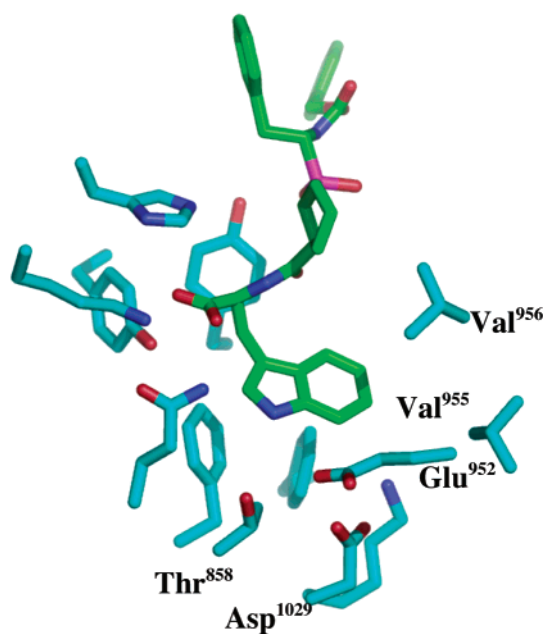


FIGURE 2: Residues forming the S_2' subsite of the C-domain of somatic ACE were defined as those located at a distance shorter than 5 Å from the RXPA380 tryptophan side chain. For clarity, residues His⁹⁵⁹ and Glu⁹⁶⁰ are omitted. Numbered residues were those changing between C-domain and N-domain. RXPA380 is colored by atom type, the carbon atoms being in green. The S_2' side chains are colored by atom type, the carbon atoms being in cyan. Hydrogen atoms are omitted. The figure was prepared with PyMOL software.

control its selectivity (Figure 2). The pseudo-proline side chain is surrounded by the carbonyl of Ala³⁵⁴ and the side chain of His³⁵³. These two residues belong to a stretch of amino acids that is highly conserved in the N- and C-domains of somatic ACE. Thus, interactions of the pseudo-proline of RXPA380 with this part of the S_1' cavity should be similar between the N- and C-domains of ACE and cannot account for the selectivity of RXPA380. Therefore, the selectivity of RXPA380 might be explained by specific interactions involving the S_2' subsite. The residues forming the S_2' subsite of the C-domain of ACE were defined as those located at a distance shorter than 5 Å from the RXPA380 tryptophan side chain in the model (Figure 2 and Table 2). On the basis of

Table 2: Comparison of the Residues between the N- and C-Domains of Somatic Human ACE Delineating the S_2' Subsite

N-domain	C-domain	N-domain	C-domain	N-domain	C-domain
Gln 259	Gln 857	Thr 358	Val 956	Phe 438	Phe 1036
Ser 260	Thr 858	Asp 393	Asp 991	Tyr 498	Tyr 1096
Asp 354	Glu 952	Glu 431	Asp 1029	Tyr 501	Tyr 1099
Ser 357	Val 955	Phe 435	Phe 1033	Phe 505	Phe 1103

this definition, several residues that surrounded the tryptophan of RXPA380 were observed to change between the N- and C-domains of somatic ACE (Table 2). Of the twelve residues listed in Table 2, only seven are strictly conserved between the N- and C-domains. Examination of the model suggests that significant changes in the S_2' subsite are the replacement of two bulky and hydrophobic residues, Val⁹⁵⁵ and Val⁹⁵⁶, in the C-domain by two smaller and polar residues, Ser³⁵⁷ and Thr³⁵⁸, in the N-domain. Such a difference in the S_2' subsite composition between the N- and C-domains suggests that the low affinity of RXPA380 for the N-domain is not due to a more restricted size of its S_2' subsite that would prevent the accommodation of the inhibitor tryptophan side chain. A more likely hypothesis could be that the favorable interactions between the tryptophan side chain and those of Val⁹⁵⁵ and Val⁹⁵⁶ in the C-domain are lost in the N-domain, due to the replacement of these valine residues by Ser³⁵⁷ and Thr³⁵⁸ in the N-domain. In the RXPA380–ACE model, the proximity between the inhibitor tryptophan side chain and Asp¹⁰²⁹ in the C-domain suggests the possible occurrence of a hydrogen bond between the NH indole ring and the carboxylate of Asp¹⁰²⁹. Replacement Asp¹⁰²⁹ in the C-domain by Glu⁴³¹ in the N-domain may lower the affinity of RXPA380 for the N-domain by decreasing the strength of this interaction. Before the development of RXPA380, it was proposed that the presence of hydrophobic residues in the P_2' position of the ACE inhibitor should enhance their selectivity for the C-domain (22). This proposal fits well with the selectivity displayed by RXPA380, as well as with the presence of two valines in the S_2' subsite of the ACE C-domain. However, as compared to several ACE inhibitors containing hydrophobic side chains in the P_2' position, the reasons for the remarkable selectivity of RXPA380 remain uncertain. The presence of the pseudo-proline in RXPA380 may impose a particular orientation to the tryptophan side chain that determines the inhibitor selectivity. Definitive clues will require the determination of the crystal structure of RXPA380 in complex with the N- and C-domains (or germinal ACE) of somatic ACE, as well as mutation experiments to complete the structural analysis.

In the lisinopril complex, the α -NH group of the lysine residue is hydrogen bound to the carbonyl group of Ala³⁵⁴ (Figure 1). The presence of a pseudo-proline in RXPA380 prevents the formation of such a hydrogen bond. The absence of this hydrogen bond should compromise the potency of RXPA380. However, the rather good potency of RXPA380 suggests that the lack of this hydrogen bond contribution to the free energy of the enzyme–inhibitor complex might be counterbalanced by the conformational constraints imposed by the pseudo-proline on the RXPA380 conformation in the free state. Indeed, as discussed above, the conformation of RXPA380 seems to fit well the structural requirements of the ACE active site.

Identification of the first N-domain-selective inhibitor of somatic ACE was achieved by screening of phosphinic peptide libraries. The development of RXPA380 was based on studies showing that some bradykinin-potentiating peptides exhibit selectivity for the C-domain of ACE (14). The resolution of the 3D structure of germinal ACE offers the structural framework for a structure-based design approach. According to our model, substitution of the β -carbon of pseudo-proline by alkylamino groups would permit development of new inhibitors that will mimic the lysine interactions of lisinopril (Figure 1). This model can also be used to drive mutation experiments aimed at demonstrating the role of particular residues in the ACE active site. As recently discussed by Acharya et al. (6), there are still many important issues to address if we are to uncover the structural basis of somatic ACE selectivity. These include the relation between chloride binding and the position of the N-terminal "lid" and the degree of interaction between the N- and C-domains in somatic ACE. Our recent results showing that the inhibition of either the N- or C-domain of somatic ACE prevents the cleavage of Ang I, but not that of bradykinin, call for the development of somatic ACE models or structures that can be used to resolve these issues (10). The recent discovery that somatic ACE functions as a receptor which mediates outside-in signaling (23) also raises interesting issues. The authors observed that inhibitors of ACE, such as perindopril, but also bradykinin and not angiotensin I, are able to promote an outside-in signaling. The mechanisms by which the binding of ligands (inhibitor or substrate) to the extracellular domain of ACE triggers intracellular events remain elusive, but suggest that the somatic ACE structure may undergo complex conformational shifts that are critical for its function. Interestingly, comparison of the ACE2 structure between the free and inhibitor-bound states reveals a large hinge binding motion (24). Similar conformational changes are expected to occur in ACE upon inhibitor binding. Selective inhibitors of ACE should be valuable tools to unveil the details of the ACE structure that might be critical to control its function.

SUPPORTING INFORMATION AVAILABLE

Further spectroscopic and analytical data of all new pseudo-proline phosphinic synthetic intermediates and full spectroscopic data for RXPA380. This material is available free of charge via the Internet at <http://pubs.acs.org>.

REFERENCES

1. Erdos, E. G. (1990) Angiotensin I converting enzyme and the changes in our concepts through the years. Lewis K. Dahl memorial lecture, *Hypertension* 16, 363–70.
2. Bhoola, K. D., Figueroa, C. D., and Worthy, K. (1992) Bioregulation of kinins: kallikreins, kininogens, and kininases, *Pharmacol. Rev.* 44, 1–80.
3. Gavras, H. (1994) Corcoran Lecture. Angiotensin-converting enzyme inhibition and the heart, *Hypertension* 23, 813–8.
4. Dzau, V. J. (2001) Theodore Cooper Lecture: Tissue angiotensin and pathobiology of vascular disease: a unifying hypothesis, *Hypertension* 37, 1047–52.
5. Zaman, M. A., Oparil, S., and Calhoun, D. A. (2002) Drugs targeting the renin-angiotensin-aldosterone system, *Nat. Rev. Drug Discov.* 1, 621–36.
6. Acharya, K. R., Sturrock, E. D., Riordan, J. F., and Ehlers, M. R. (2003) Ace revisited: a new target for structure-based drug design, *Nat. Rev. Drug Discov.* 2, 891–902.
7. Soubrier, F., Alhenc-Gelas, F., Hubert, C., Allegrini, J., John, M., Tregear, G., and Corvol, P. (1988) Two putative active centers in human angiotensin I-converting enzyme revealed by molecular cloning, *Proc. Natl. Acad. Sci. U.S.A.* 85, 9386–90.
8. Wei, L., Alhenc-Gelas, F., Corvol, P., and Clauser, E. (1991) The two homologous domains of human angiotensin I-converting enzyme are both catalytically active, *J. Biol. Chem.* 266, 9002–8.
9. Dive, V., Cotton, J., Yiotakis, A., Michaud, A., Vassiliou, S., Jiracek, J., Vazeux, G., Chauvet, M. T., Cuniasse, P., and Corvol, P. (1999) RXP 407, a phosphinic peptide, is a potent inhibitor of angiotensin I converting enzyme able to differentiate between its two active sites, *Proc. Natl. Acad. Sci. U.S.A.* 96, 4330–5.
10. Georgiadis, D., Beau, F., Czarny, B., Cotton, J., Yiotakis, A., and Dive, V. (2003) Roles of the two active sites of somatic angiotensin-converting enzyme in the cleavage of angiotensin I and bradykinin: insights from selective inhibitors, *Circ. Res.* 93, 148–54.
11. Candido, R., Jandeleit-Dahm, K. A., Cao, Z., Nesteroff, S. P., Burns, W. C., Twigg, S. M., Dilley, R. J., Cooper, M. E., and Allen, T. J. (2002) Prevention of accelerated atherosclerosis by angiotensin-converting enzyme inhibition in diabetic apolipoprotein E-deficient mice, *Circulation* 106, 246–53.
12. Natesh, R., Schwager, S. L., Sturrock, E. D., and Acharya, K. R. (2003) Crystal structure of the human angiotensin-converting enzyme-lisinopril complex, *Nature* 421, 551–4.
13. Ehlers, M. R., Fox, E. A., Strydom, D. J., and Riordan, J. F. (1989) Molecular cloning of human germinal angiotensin-converting enzyme: the testis isozyme is identical to the C-terminal half of endothelial angiotensin-converting enzyme, *Proc. Natl. Acad. Sci. U.S.A.* 86, 7741–5.
14. Cotton, J., Hayashi, M. A., Cuniasse, P., Vazeux, G., Ianzer, D., De Camargo, A. C., and Dive, V. (2002) Selective inhibition of the C-domain of angiotensin I converting enzyme by bradykinin potentiating peptides, *Biochemistry* 41, 6065–71.
15. Baylis, E. K., Cambell, M., and Dingwall, J. G. (1984) 1-aminoalkylphosphonous acids. part 1. isosteres of the protein aminoacids, *J. Chem. Soc., Perkin Trans. 1* 2845–853.
16. Yiotakis, A., Vassiliou, S., Jiracek, J., and Dive, V. (1996) Protection of the Hydroxyphosphinyl Function of Phosphinic Dipeptides by Adamantyl. Application to the Solid-Phase Synthesis of Phosphinic Peptides, *J. Org. Chem.* 61, 6601–6605.
17. Brooks, B. R., Bruccoleri, R. E., Olafson, B. D., States, D. J., Swaminathan, S., and Karplus, M. (1983) *J. Comput. Chem.* 4, 187–217.
18. MacKerell, A. D., Bashford, D., Bellott, M., Dunbrack, R. L., Evanseck, J. D., Field, M. J., Fischer, S., Gao, J., Guo, H., Ha, S., Joseph-McCarthy, D., Kucunhir, L., Kuczera, K., Lau, F. T. K., Mattos, C., Michnick, S., Ngo, T., Nguyen, D. T., Prodhom, B., Reiher, W. E., Roux, B., Schlenkrick, M., Smith, J. C., Stote, R., Straub, J., Watanabe, M., Wiorkiewicz-Kuczera, J., Yin, D., and Karplus, M. (1998) *J. Phys. Chem. B* 102, 3586–3616.
19. Frisch, M. J., Trucks, G. W., Schlegel, H. B., Scuseria, G. E., Robb, M. A., Cheeseman, J. R., Zakrzewski, V. G., Montgomery, J. A., Stratmann, R. E., Burant, J. C., Dapprich, S., Millam, J. M., Daniels, A. D., Kudin, K. N., Strain, M. C., Farkas, O., Tomasi, J., Barone, V., Cossi, M., Cammi, R., Mennucci, B., Pomelli, C., Adamo, C., Clifford, S., Ochterski, J., Petersson, G. A., Ayala, P. Y., Cui, Q., Morokuma, K., Salvador, P., Dannenberg, J. J., Malick, D. K., Rabuck, A. D., Raghavachari, K., Foresman, J. B., Cioslowski, J., Ortiz, J. V., Baboul, A. G., Stefanov, B. B., Liu, G., Liashenko, A., Piskorz, P., Komaromi, R., Gomperts, R., Martin, R. L., Fox, D. J., Keith, T., Al-Laham, M. A., Peng, C. Y., Nanayakkara, A., Challacombe, M., Gill, P. M. W., Johnson, B., Chen, W., Wong, M. W., Andres, J. L., Gonzalez, C., Head-Gordon, M., Replogle, E. S., and Pople, J. A. (2002) Gaussian 98 (Revision A.11.3), Gaussian Inc., Pittsburgh, PA.
20. Moritani, Y., Fukushima, C., Miyagishima, T., Ohmizu, H., and Iwasaki, T. (1996) Simple synthesis of trans- α,β -dibenzyl- γ -butyrolactone lignans by diastereoselective reduction of α -benzylidene- β -benzyl- γ -butyrolactones using NaBH₄–NiCl₂, *Bull. Chem. Soc. Jpn.* 69, 2281–2286.
21. Cushman, D. W., Cheung, H. S., Sabo, E. F., and Ondetti, M. A. (1977) Design of potent competitive inhibitors of angiotensin-converting enzyme. Carboxyalkanoyl and mercaptoalkanoyl amino acids, *Biochemistry* 16, 5484–91.
22. Perich, R. B., Jackson, B., and Johnston, C. I. (1994) Structural constraints of inhibitors for binding at two active sites on somatic angiotensin converting enzyme, *Eur. J. Pharmacol.* 266, 201–11.

23. Kohlstedt, K., Brandes, R. P., Muller-Esterl, W., Busse, R., and Fleming, I. (2004) Angiotensin-converting enzyme is involved in outside-in signaling in endothelial cells, *Circ. Res.* 94, 60–7.
24. Towler, P., Staker, B., Prasad, S. G., Menon, S., Tang, J., Parsons, T., Ryan, D., Fisher, M., Williams, D., Dales, N. A., Patane, M.

A., and Pantoliano, M. W. (2004) ACE2 structures reveal a large hinge-bending motion important for inhibitor binding and catalysis, *J. Biol. Chem.* 279, 17996–07.

BI049504Q